

This version of the ESI published 11 July 2024 replaces the original version published 8 July 2024 as the references in Table S2 were incorrect.

Electronic Supplementary Material (ESI) for RSC Advances

Study of the correlation between magnetic and electrical properties of the $\text{La}_{0.6}\text{Sr}_{0.4}\text{MnO}_3$ compound

H. Gharsallah ^{a,b}, M. Jeddi ^a, M. Bejar ^{a,c,*}, E. Dhahri ^a, S. Nouari ^d

^a Laboratoire de Physique Appliquée, Faculté des Sciences, B.P. 1171, 3000 Sfax, Université de Sfax, Tunisie.

^b Institut Préparatoire aux Études d'Ingénieur de Sfax, BP 1172-3018 Sfax, Université de Sfax, Tunisie.

^c Faculté des Sciences de Monastir, Avenue de l'environnement 5019 Monastir, Université de Monastir, Tunisie.

^d Department of mechanical engineering, King Fahd University of Petroleum and Minerals, Dhahran, Saudi Arabia.

Contents

[Table S1](#): Refined structural parameters for $\text{La}_{0.6}\text{Sr}_{0.4}\text{MnO}_3$ (S1C0).

[Table S2](#): Comparison of the magneto transport properties of $\text{La}_{0.6}\text{Sr}_{0.4}\text{MnO}_3$ (S1C0) with other materials.

[Fig. S1](#): The temperature dependence of the inverse of the magnetic susceptibility.

[Fig. S2](#): The variations according to the temperature of the magnetization $M(T)$ and the electrical resistance $R(T)$ under different applied magnetic fields.

[Fig. S3](#) : Fit of the temperature dependence of resistance, at low temperatures, with the

three models: **(a)** the (ZDE) polynomial $R(T) = R_0 + R_2T^2 + R_{4.5}T^{4.5}$ model with (e-m)

interactions, **(b)** the (ZDE) polynomial $R(T) = R_0 + R_2T^2 + R_5T^5$ model with (e-ph)

scattering, and **(c)** the (SPCM)
$$R(T) = R_0 + \frac{R_2}{\sinh^2\left(\frac{T_2}{T}\right)} + R_nT^n$$
 model.

This version of the ESI published 11 July 2024 replaces the original version published 8 July 2024 as the references in Table S2 were incorrect.

Fig. S4: Fit of the temperature dependence of resistance $R(T)$, at high temperatures, with the four transport models: **(a)** The (TAH), **(b)** the adiabatic (SPH), **(c)** the non-adiabatic (SPH) and **(d)** the (VRH).

Table S1: Refined structural parameters for $La_{0.6}Sr_{0.4}MnO_3$ (S1C0).

Space group	<i>P bnm</i> 100.00 (1.72) $a \neq b \neq c$ $\alpha = \beta = \gamma = 90^\circ$
<i>a</i> (Å)	5.502 ₅
<i>b</i> (Å)	5.457 ₃
<i>c</i> (Å)	7.727 ₄
<i>La, Ca, Sr sites</i> (<i>x, y, z</i>) <i>Mult</i> = 4	0.997 ₇ 0.018 ₈ 0.25
<i>Mn site</i> (<i>x, y, z</i>) <i>Mult</i> = 4	0.50 0.00 0.00
<i>O₁</i> (<i>x, y, z</i>) <i>Mult</i> = 4	0.075 ₇ 0.513 ₅ 0.25
<i>O₂</i> (<i>x, y, z</i>) <i>Mult</i> = 8	<i>Mult</i> = 8 0.711 ₄ 0.289 ₀ 0.015 ₆
<i>V</i> (Å ³)	58.012
<i>Mn-O₁-Mn</i> (°)	155
<i>Mn-O₂-Mn</i> (°)	161
<i>d_{Mn-O₁}</i> (Å)	1.97 ₇
<i>d_{Mn-O₂}</i> (Å)	1.96 ₃
$\langle d_{Mn-O} \rangle$ (Å)	1.96 ₇
$\sigma^2 \langle Mn-O \rangle$	6.5546×10^{-5}
<i>R_F</i> (%)	3.90
<i>R_B</i> (%)	2.69
<i>R_p</i> (%)	13.5
<i>R_{wp}</i> (%)	9.95
<i>R_{exp}</i> (%)	6.12
χ^2 (%)	2.64

This version of the ESI published 11 July 2024 replaces the original version published 8 July 2024 as the references in Table S2 were incorrect.

Table S2: Comparison of the magneto transport properties of $\text{La}_{0.6}\text{Sr}_{0.4}\text{MnO}_3$ (S1C0) with other materials.

Compound	$\mu_0 H$ (T)	T_R (K)	MR_{max} (%)	$ TCR(\%) _{max}$	References
$\text{La}_{0.6}\text{Sr}_{0.4}\text{MnO}_3$	2	222	20.1	0.84	This work
$\text{Nd}_{0.6}\text{Sr}_{0.3}\text{K}_{0.1}\text{MnO}_3$		221	39	1.3	[45]
$\text{La}_{0.7}\text{Ca}_{0.25}\text{Sr}_{0.05}\text{MnO}_3$	0.1	259	15.4		[47]
$\text{La}_{0.7}\text{Ca}_{0.15}\text{Sr}_{0.15}\text{MnO}_3$		263	14.2		[47]
$\text{La}_{0.7}\text{Ca}_{0.1}\text{Sr}_{0.2}\text{MnO}_3$		269	18.1		[47]
$\text{La}_{0.7}\text{Ca}_{0.3}\text{MnO}_3$	1	172	25		[48]
$\text{La}_{0.7}\text{Ca}_{0.2}\text{Ag}_{0.1}\text{MnO}_3$		200	30		[48]
$\text{La}_{0.7}\text{Ca}_{0.1}\text{Ag}_{0.2}\text{MnO}_3$		296	20.8		[48]
$\text{La}_{0.7}\text{Ag}_{0.3}\text{MnO}_3$		303	17.1		[48]
$\text{La}_{0.75}\text{Sr}_{0.25}\text{Mn}_{0.75}\text{Cr}_{0.25}\text{O}_3$	2	228	62		[46]
$\text{La}_{0.6}\text{Sr}_{0.25}\text{K}_{0.15}\text{MnO}_3$		287	45		[52]
$\text{La}_{0.6}\text{Ca}_{0.4}\text{MnO}_3$		220	45	1.3	[53]
$\text{La}_{0.5}\text{Ag}_{0.1}\text{Ca}_{0.4}\text{MnO}_3$		380		2.1	[54]
$\text{La}_{0.6}\text{Eu}_{0.1}\text{Sr}_{0.3}\text{MnO}_3$		360		1.1	[55]

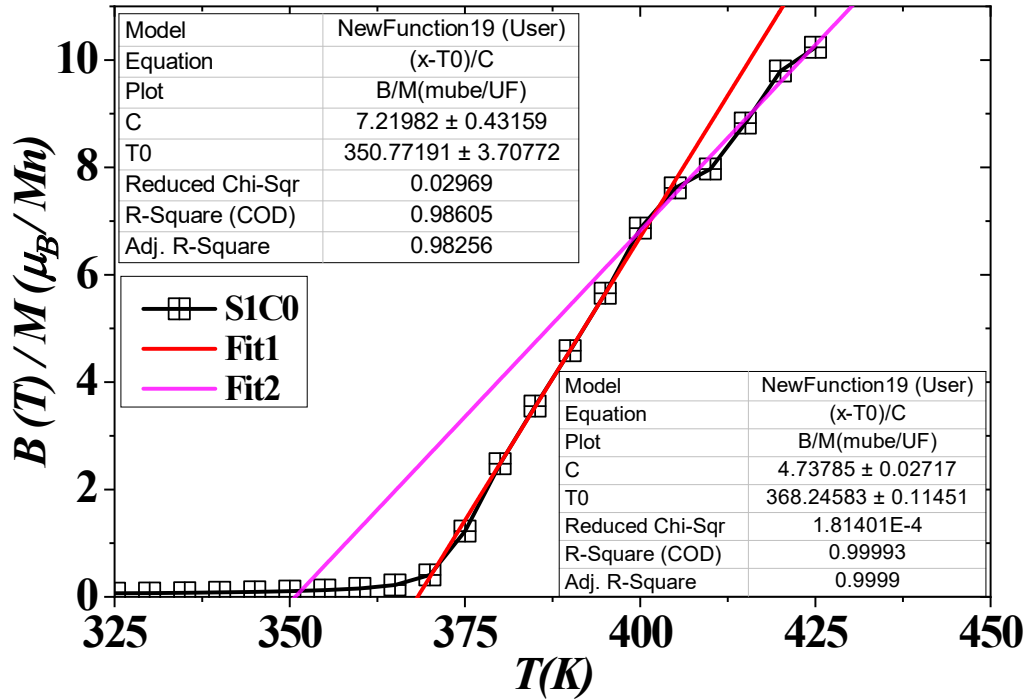
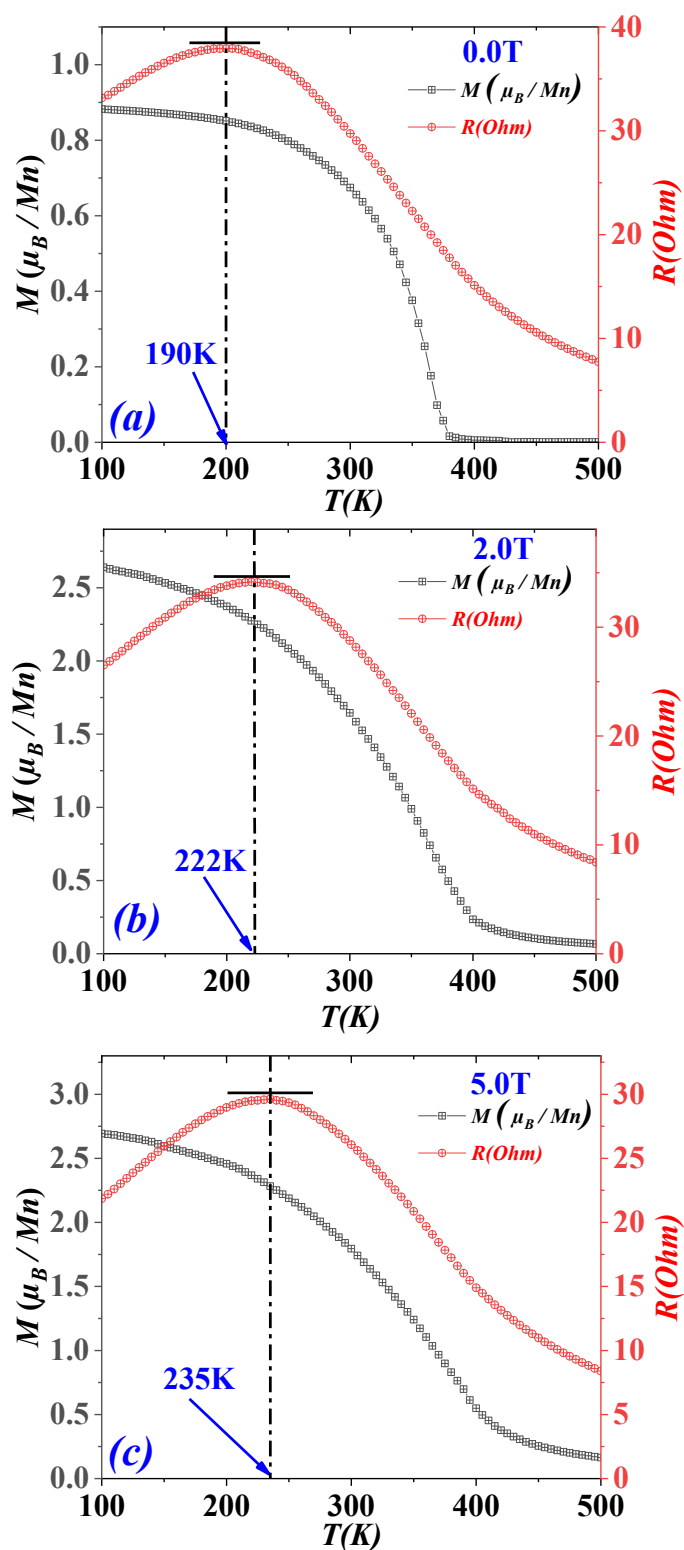
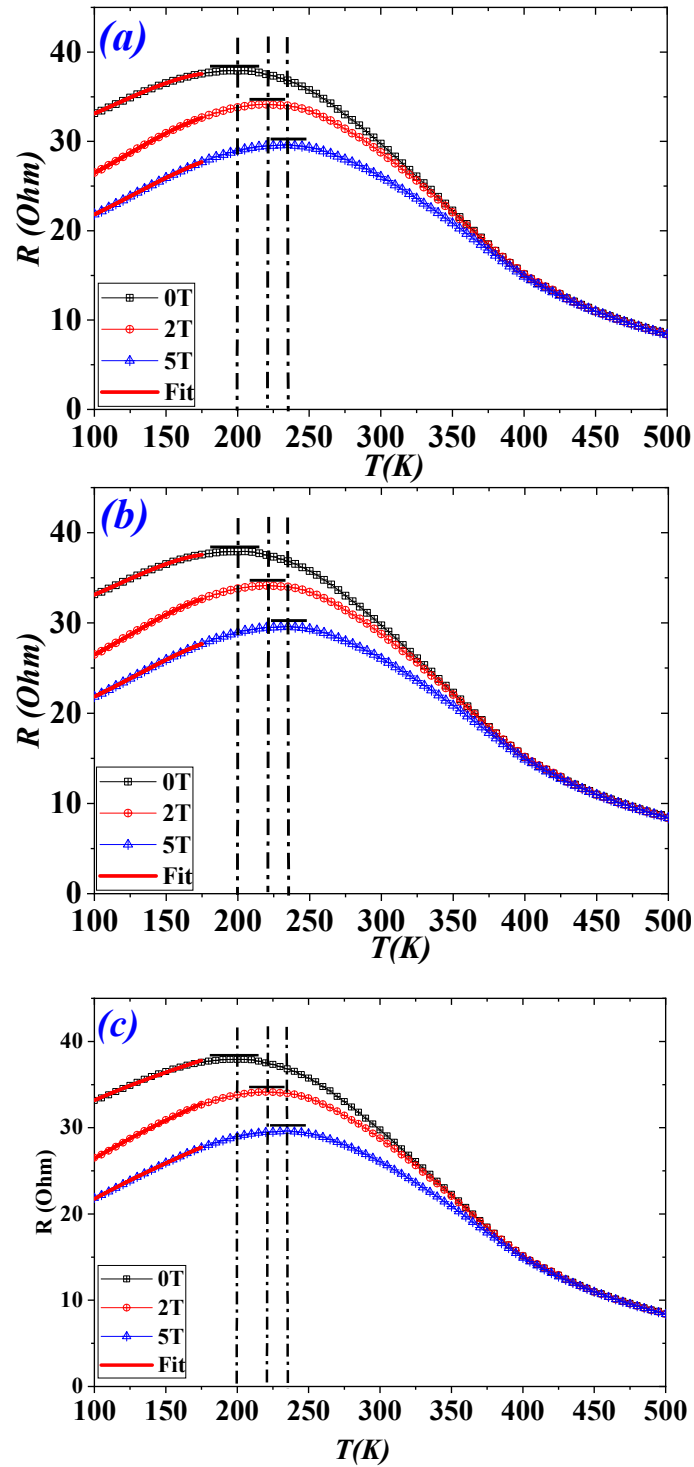


Fig. S1: The temperature dependence of the inverse of the magnetic susceptibility. The $\chi^{-1}(T)$ curve presents two linear branches. The first one is fitted with the Curie-Weiss law [31], indicating the PM-FM transition at $\theta_{WC} = 368 K$ value quite equal to the Curie temperature $T_c \approx 365 K$. The second branch, shows the existence of another temperature characteristic of the magnetic properties $T_i \approx 350 K$, indicating the existence of (*SPM*) clusters within the (*FM*) phase in the temperature interval between T_B and T_c . So, the irreversibility temperature T_i can be defined as the temperature of a *SPM/PM* transition.



Figs. S2 (a), (b) and (c) the variations according to the temperature of the magnetization $M(T)$ and the electrical resistance $R(T)$ of (S1C0) under different applied magnetic fields of 0, 2 and 5 T, respectively.



Figs. S3 : (a), (b) and (c) Fit of the temperature dependence of resistance, at low temperatures, under different applied magnetic fields of 0, 2 and 5 T, with the three models: (a) the (ZDE) polynomial $R(T) = R_0 + R_2T^2 + R_{4.5}T^{4.5}$ model with (e-m)

interactions, **(b)** the (ZDE) polynomial $R(T) = R_0 + R_2T^2 + R_5T^5$ model with (e-ph)

$$R(T) = R_0 + \frac{R_2}{\sinh^2\left(\frac{T_2}{T}\right)} + R_nT^n$$

scattering, and **(c)** the (SPCM)

model.

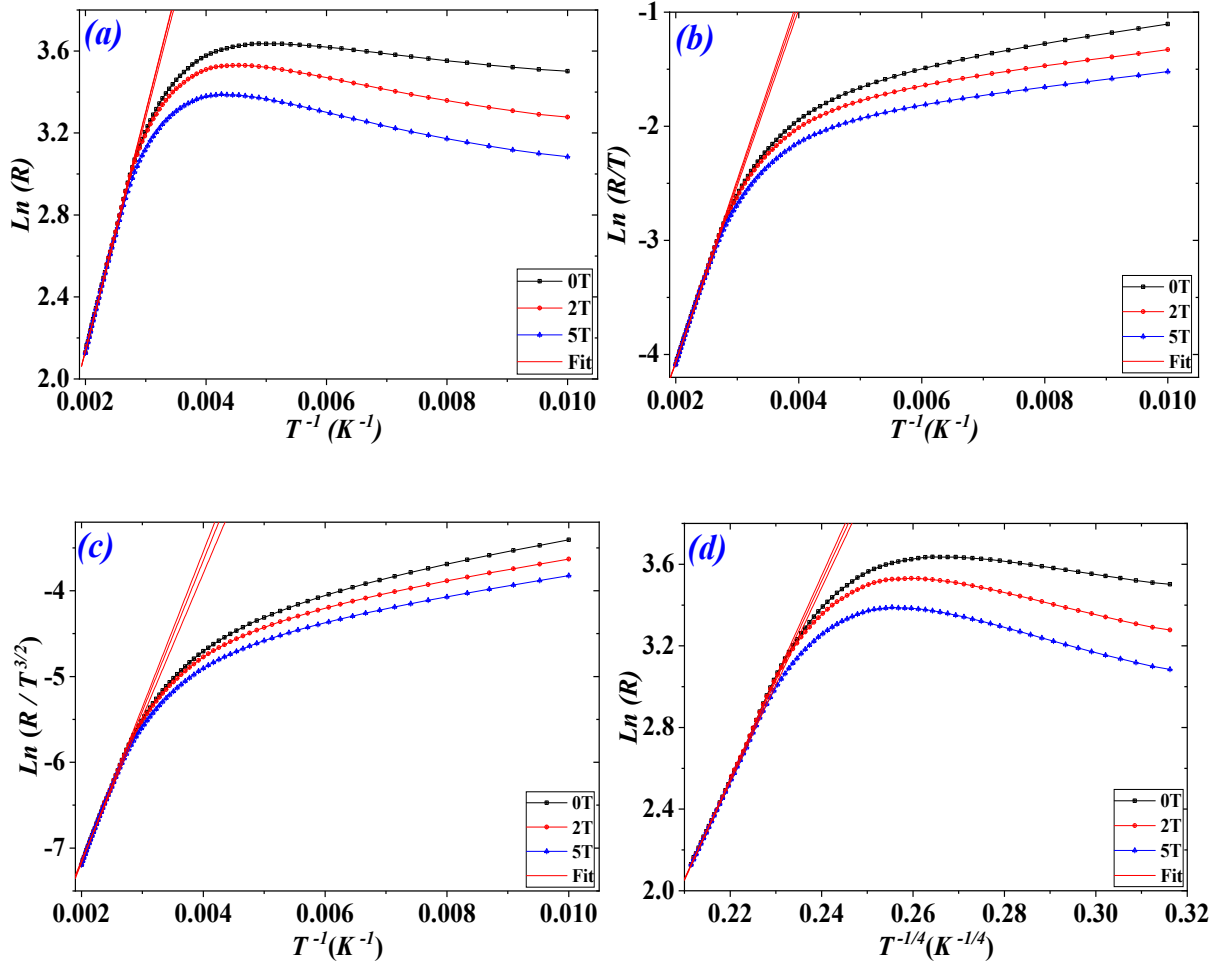


Fig. S4: Fit of the temperature dependence of resistance $R(T)$, at high temperatures, under different applied magnetic fields of 0, 2 and 5 T, with the four transport models: **(a)** The (TAH), **(b)** the adiabatic (SPH), **(c)** the non-adiabatic (SPH) and **(d)** the (VRH).